This is a repository copy of *Experimental observation of the nonlinear coupling of flame flow and acoustic wave*.

White Rose Research Online URL for this paper:
http://eprints.whiterose.ac.uk/90867/

Version: Accepted Version

Experimental observation of the nonlinear coupling of flame flow and acoustic wave

Li-Wei Chen*[a] and Yang Zhang[b]

[a] *Department of Mechanical and Computer-Aided Engineering, The National Formosa University, Yunlin, 632, Taiwan*
[b] *Mechanical Engineering Department, The University of Sheffield, Mapping Street, Sheffield S1 3JD, UK*
*Corresponding author: Phone: +886(5)6315315; Fax: +886(5)6315310; E-mail: liwei@nfu.edu.tw

Abstract

This is an experimental investigation to study the nonlinear coupling characteristics of a propane/air flame with acoustic standing waves, using chemiluminescence emission and phase-locked PIV measurements. A variety of coupling modes are observed for the excitation source with combustion instability oscillations and its harmonics and sub-harmonics. The frequency analysis shows that flame/acoustic coupling behaviour results in complex nonlinear coupling. The coupling behaviour is weak at lower excitation intensities (0.3V). At a voltage amplitude of 2 V, the results show that the excitation frequency (f_e) is only coupled with the sub-harmonic frequency ($f_e/5$) for the premixed flame. However, for the diffusion flame, more complex frequency components are observed, which exhibit relationships of $f_e \pm f_f$ and $f_e \pm f_e/5$. At a voltage amplitude of 13.7 V, the sub-harmonic frequencies ($2f_e/5$ and $3f_e/5$) and the premixed flame buoyancy oscillations (f_f) are increased. PIV measurements provide detailed flow velocity vector fields in an acoustically excited tube for different phase angles and the effect on the flames at different equivalence ratios, which increases the understanding of flame oscillation behaviour. It is found that all of the nonlinear phenomena that are observed occur because of the coupling between buoyant and acoustic excitation and create complex nonlinear frequency couplings.

***Keywords**: Flame/acoustic wave interaction; standing wave; nonlinear coupling; PIV.*

1. Introduction

Combustion instability is commonly observed in practical combustion systems, such as furnaces and gas turbines. Flame-acoustic interaction is one of the major reasons for these undesirable phenomena in an enclosed combustion system. It is known that the range of acoustic frequencies, amplitudes and phase angles can affect the flame dynamics. Due to the thermoacoustic mechanism, the amplitude of acoustic oscillations can grow and therefore their effect on the flame dynamics also grows [1, 2]. These effects are enhanced in a combustion chamber, because there is coupling between an unsteady heat-release rate and acoustic pressure. Under certain conditions, this coupling can result in increased thermoacoustic instability oscillations and consequently lead to failure of the system [3, 4]. Practically, these unstable processes occur in the nonlinear regime, where the system oscillates at a limit cycle [5]. Determining the mechanism of thermoacoustic instability is complex because it involves a number of different phenomena.

It is seen that flame dynamics are significantly altered by acoustic excitation. Acoustically excited flames are useful for research involving flame-acoustic interactions because acoustic perturbation is an advantageous means of control for a flame that oscillates at specific frequencies [6]. The acoustic signal can also be synchronised with other measurement devices. Depending on the frequency and magnitude, the addition of a forced acoustic field can considerably modify the dynamic flame structures and movements. The use of external acoustic perturbation also has an effect on combustion at the chemical level, which results in a change in the emissions and the molecular concentrations [7, 8]. There have been many studies of nonlinear flame oscillations using acoustically excited flames. Kim et al. [8] and Kartheekeyan et al. [9] demonstrated that external forcing an induced flame periodic oscillation can further create undesirable nonlinear oscillations that affect the initial flow velocity and the mixing rate for a premixed flame. Experimental work has

shown that flames exhibit nonlinear responses under various acoustic and combustion conditions. In nonlinear systems, the flame oscillation wave and the acoustic excitation wave can induce other frequency components, besides the excitation frequency. For instance, a sub-harmonic flame response was found in pulsed premixed methane/air flames in the studies by Bourehla and Baillot [10]; and Williams et al. [11] showed the existence of sub-harmonic flame oscillation components of $f/2$, $f/3$, $2f/3$, $f/4$ and $f/5$ in a laser-based investigation of the structures of a acoustically excited flame. Huang et al. [12] identified nonlinear couplings between the buoyancy driven flame instability and acoustic excitation using high speed colour imaging and an innovative colour digital image processing technique for an acoustically excited and baffle-stabilised diffusion flame burner.

Most of these studies concentrate on external excitation in a fuel pipe in an open space. Not many studies involve the observation of nonlinear flame dynamics in an acoustically forced tube and their coupling behaviour. Recently, the authors have used a phase-locked PIV system to study the flow characteristics for a propane diffusion flame at different nozzle position along an acoustically excited tube [13]. The results show that the diffusion flame dynamics are significantly affected by the standing wave in a tube because of the large velocity oscillation in the acoustic flow in the anti-node area. The main objective of this study is to use nonlinear theory to explain the observed nonlinear response modes for an acoustically excited premixed flame in a tube. A chemiluminescence emission measurement system (PMT) is used to systematically examine the oscillating frequency of propane-air flames at different intensities of acoustic excitation, especially the nonlinear coupling of the flame dynamics and acoustic excitation. Detailed flame flow velocity fields and vorticity are measured and calculated using a PIV (Particle Image Velocimetry) system, to make use of more useful physical flame parameters from the two-dimensional spatial information and to further understand the flame/acoustic coupling behaviour.

2. Experimental Setup

The schematic layout of the experimental apparatus is illustrated in Fig. 1. The design is similar to the design in reference [13]. It consists of a burner system, a computer controlled 3D traverse, a signal generation and a synchronisation system, a PIV system and a chemiluminescence emission measurement system (PMT). The square tube was used to simulate the enclosed environment of a practical combustion chamber. The burner utilised in this study was designed to produce a wide range of premixed stabilised flames. Gaseous fuel (Propane) and air were respectively supplied from the fuel bottle and the compressed air bottle and were controlled by dedicated flow-meters. The flow rate for the propane was set at 55ml/min. Using this fuel flow rate, three equivalence ratios of premixed flames were set as the main parameters. The experimental conditions are listed in table 1. External acoustic excitation was provided by a loudspeaker, which was driven by a power amplifier whose amplitude and frequency signals were controlled by a PC base LabView system. The driving amplitude was defined using the peak-to-peak of the output voltage (V) of the amplifier and was set at 0.3V, 2V and 13.7V for the study. The details for the burner system, the PIV system and the signal generation and synchronisation system are the same as those for [13]. The chemiluminescence emission measurement apparatus consisted of two photomultipliers (ORIEL, Model: 70704), a high voltage source supply, a converging lens arrangement, optical filters and a randomly bifurcated fine fibre optic bundle. This optical system measured the flame chemiluminescence intensity using a photomultiplier-tube (PMT). The filtered light collected from the flame was used a set of monochromatic filters. Transmission of the light signal was accomplished using a fibre optic cable. The CH* chemiluminescence was collected using a lens system, which was designed to image the flame onto the end of a fibre optic cable. The data outputs from the multipliers were displayed and stored in a PC based system. A National Instruments DAQ card and LabVIEW software were then used for data acquisition, monitoring and

analysis. The acoustic excitation signal, the PIV trigger timing and the PMT signals were synchronized to allow a logical analysis.

3. Results and Discussion

Previous research [14] proved that the first four resonance frequencies of the present rig were 65 Hz, 220 Hz, 385 Hz and 550 Hz, respectively. The acoustical node and anti-node regions also fit the observable area for the current test rig at an external excitation frequency of 385 Hz. Therefore, an acoustic excitation frequency of 385 Hz was set as the main frequency for further analysis. The burner nozzle was positioned in the acoustic anti-node region (see Fig. 1) to determine how the flame wave responded nonlinearly to acoustic excitation. Figure 2 shows the visible flame images at different equivalence ratios at an excitation frequency of 385 Hz and a voltage amplitude of 13.7 V (2 V in the case of $\emptyset$ = 1.5). The strongly oscillating diffusion flame case is also shown in Fig. 2a. It is seen that under the same acoustic excitation, the premixed flame is more stable than a diffusion flame. The flame pattern is also more stable when the air-fuel mixing ratio is increased. At an equivalence ratio of 5, a reddish flame colour is only visible at the flame tip. The flame oscillation behaviour is similar to that for the diffusion flame, but it is much weaker. At $\emptyset$ = 1.5, which is the flammability limit for the current nozzle, the flame oscillation is the weakest of all the test cases. The flame cone angle remains almost constant under acoustic forcing. However, the flame can be extinguished suddenly by a slight increase in amplitude. These observations demonstrate that the behaviour of the premixed flame is quite different to that for a diffusion flame under acoustic perturbation. A diffusion flame can become a lifted flame, a partially premixed flame or a partially extinct flame type, during each flame oscillation cycle.

In the case of the premixed flame, the flame pattern is generally stable and only a slight oscillation is observed when there is external excitation. For $\emptyset$ = 3, Fig. 2c shows that the flame bottom is

attached to the nozzle in the 2nd image and then the flame is partially lifted. After that, the visible blue flame pattern is observed below nozzle exit. This occurs because when the acoustic flow is downward, the flame is pushed by the acoustic wave. In contrast, the flame slightly lifts off when the acoustic flow is turned upwards. This study also found that this kind of flame behaviour is not observable at $\emptyset$ = 1.5. As shown in Table 1, the initial mean nozzle exit velocity at $\emptyset$ = 1.5 is 1.28 m/s, which is higher than that for the other cases. This is much higher than the largest downward acoustic flow velocity, which is around 0.6 m/s. It is seen that for the extreme case, the fuel jet still resists the downward acoustic wave. Therefore the flame is stable at each phase angle of the excitation cycle. However, the flame is close to the lower flammable limit at $\emptyset$ = 1.5, so the mixture is probably further diluted by the acoustic perturbation. It is eventually extinguished when there is a slight increase the excitation intensity.

Figure 3 illustrates the power spectrum for the CH* chemiluminescence signals for the premixed flames under acoustic excitation. The frequency components are very different at the different equivalence ratios and external excitation intensities. For the case of a premixed flame, at a voltage amplitude of 0.3 V, the only visible peak is the forcing frequency. For the diffusion flame ($\emptyset$ = ∞), both the flame flickering frequency (f_f = 15 Hz) and the forcing frequency (f_e = 385 Hz) are observed. The harmonic frequencies of the natural flame frequency are also observed at 0.3 V. An expanded view of the excitation frequency peak region shows two small peaks, which exhibit a relationship of $f_e \pm f_f$ for the case of $\emptyset$ = ∞. At voltage amplitudes of 13.7 V and 2 V, the excitation frequency is found, accompanied by two sets of fore and aft peaks. The data indicates that these complementary peaks exhibit a relationship of $f_e \pm f_f$ and $f_e \pm f_e/5$, and two clear peaks are also visible at the natural flickering frequency (f_f) and the sub-harmonic frequency of the excitation

frequency, which is $f_e/5$. Unlike the obvious flame flickering in the diffusion flame, the natural flame

flickering frequency for the premixed flame is difficult to determine and the external perturbation

intensity is sufficiently large to overshadow the low frequency buoyancy-induced flame flicker.

Therefore, the sub-harmonic frequency ($f_e/5$) is observed as the main complementary frequency

peak, instead of the flame flickering frequency. For instance, the complementary peaks are shown

to have a relationship of $f_e \pm f_e/5$ for the premixed flame at 2 V.

These frequency components are explained by nonlinear theory and they are attributed to the

nonlinear response modes. For instance, the harmonic frequencies for the natural flame frequency

for the diffusion are correlated to the nonlinear response, which is shown in below:

$$y_f(t) = Y_f sin(n\omega t + \varphi_f) \tag{1}$$

Fore and aft complementary frequency peaks at higher forcing intensities have been reported

recently by Huang et al. [12] , using a different test rig and using high speed colour imaging and

processing. They have also been observed in the nonlinear response of quasi-periodic fluid motion

[15]. Fenstermacher et al. [16] examined the turbulence transition of radial fluid velocity under

cylindrical rotational excitations using laser-Doppler velocimetry and Fourier-Transformation (FT).

The results showed the existence of a subtractive frequency-coupling component that is similar to

that of the f_e - f_f and f_e - $f_e/5$ modes. The nonlinear coupling between the $x_e(t) = X_e sin(\omega_e t)$ and

$x_f(t) = X_f sin(\omega_f t)$ or $x_{e/5}(t) = X_{e/5} sin(\omega_{e/5} t)$ wave signals can result in the creation of a

$k sin(\omega_e t) sin(\omega_f t)$ or a $k sin(\omega_e t) sin(\omega_{e/5} t)$ frequency component. This can then be broken down

into the following equations:

$$k(cos([\omega_e - \omega_f]t) - cos([\omega_e + \omega_f]t))/2 \tag{2}$$

or

7

$$k(cos([\omega_e - \omega_{e/5}]t) - cos([\omega_e + \omega_{e/5}]t))/2 \qquad (3)$$

This may explain the observed nonlinear coupling relationship of $f_e \pm f_f$ and $f_e \pm f_e/5$.

Studies of the effect of the forcing intensity show that there are no observable harmonic coupling at 0.3 V. After further increasing the voltage amplitude to 2 V, the frequency component is similar for each premixed flame and the external forcing has no obvious effect on the premixed flame at different equivalence ratios. However, the sub-harmonic frequencies, which are $2f_e/5$ and $3f_e/5$, become visible in both the diffused and premixed flame cases. A further increase in the voltage amplitude to 13.7 V produces frequency components is similar to those at 2 V, but the amplitude of the sub-harmonic response is increased. A tiny peak is also observed at around 10 Hz, at $\emptyset$ = 3 and 5. A set of fore and aft peaks that accompany each sub-harmonic frequency are also observed. The power spectrum for the premixed flame without excitation indicates that the natural flickering of the premixed flame is around 10 Hz. It is seen that the lower intensity of the acoustic excitation can overshadow the flicker frequency. However, it can be induced again at higher forcing intensities.

Figure 4 shows the velocity vectors and the vorticity contour maps for the flow field for the premixed flames at different equivalence ratios. The velocity fields for the premixed flame are similar to those for the diffusion flame at phase angles of 72° and 144°, where the acoustic wave induces an upward flow motion, which further accelerates the flame buoyancy effect for each case. The flame flow velocity was then increased to the maximum at these phase angles. At a phase angle of 0°, the acoustic perturbation is low. A strong upward flow motion is observed above the nozzle for the premixed flame and no obvious downward velocity vectors can be seen on the X-axis. The displacement of the acoustic flow motion only affects the diffusion flame because for the

diffusion flame, the fuel jet needs surrounding air as an oxidant to sustain the chemical reaction. In this case, the low initial velocity of the fuel jet and the ambient air are both affected by the acoustic excitation. There is an obvious disturbance in the flame flow pattern at a phase angle of 0°. At a phase angle of 288°, the largest downward acoustic flow is observed. The velocity field at this phase angle is very different for each flame. For the diffusion flame, the upward flame flow and the downward acoustic flow create a chaotic flow pattern, whereas for the premixed flame, upward velocity vectors are observed in the centre of each figure. When the air-fuel mixture rate is increased, the flow motion becomes stronger. For the case of $\emptyset = 5$, a cone-shaped low velocity field is observed at Z = 20 mm, where the flame front is pushed by the strong downward acoustic field. A comparison between this data and Fig. 2b shows that the mushroom-shaped flame tip in 3rd, 4th and 5th image matches the PIV velocity data. At $\emptyset = 3$, a greater air flow rate increases the initial fuel velocity and resists the downward acoustic flow, so the upward flame flow pattern on the X-axis is stronger than that for $\emptyset = 5$ at phase angles of 216° and 288°. It is seen that the combination of the initial mixture flow velocity and the buoyancy effect of the flame counters the acoustic effect.

The vorticity contour maps in Fig. 4 show that the angled velocity acceleration zones match well with the angled vorticity contour. In the diffusion flame, many disordered positive and negative vorticities are spread across the image, at each phase angle. The upwardly moving hot gas is broken up by the up-and-down flow of the acoustic wave. These locally opposing flows then form many little vortices because of Kelvin-Helmholtz instability. For the premixed flame, strong vorticity is distributed on both sides of the X-axis. The positive vorticity is shown on the left hand side and the right hand side is negative. In particular, vorticity patterns are observed at phase angles of 0°, 72° and 144°. This is because a greater initial fuel velocity is combined with strong upward movement

of hot gases and is further accelerated by upward acoustic flow. This combination creates a fast flow that is stronger than the strongest upward acoustic flow. Therefore, these two flows create relatively opposite velocity gradients and form a strong vortex. At phase angles of 216° and 288°, the flame flow is pushed by the downward acoustic flow and results in a decreased upward flame flow, so the vortex is weaker.

4. Conclusions

The nonlinear coupling response of flame dynamics and acoustic excitation in an acoustically excited standing wave tube is determined using a chemiluminescence emission measurement system and a PIV system. The acoustic excitation leads to change in the observed flame oscillation frequency and the flow structure evolutions for excitation signals of different amplitudes for different equivalence ratios.

The frequency analysis of the flame oscillation indicates that flame/acoustic coupling behaviour results in nonlinear flame dynamics. In the acoustic velocity anti-node region, both the natural flickering frequency and the excitation frequency of the flame dominate the flame behaviour for a diffusion flame at 0.3 V. For a premixed flame, excitation forcing is the only factor that affects the flame dynamics and no coupling behaviour is detected at such a low intensity. When the voltage amplitude is raised to 2 V, the excitation frequency (f_e) is accompanied by nonlinear fore and aft frequency peaks. In the premixed flame, these complementary frequency peaks are shown to have a relationship of $f_e \pm f_e/5$. For the diffusion flame, it is found that the excitation frequency is coupled with both the sub-harmonic frequency of the excitation frequency ($f_e/5$) and the natural flame oscillating frequency (f_f). At higher excitation intensities, the natural frequency and the sub-harmonic frequencies ($2f_e/5$ and $3f_e/5$) are increased. These sub-harmonic frequencies then couple

10

with the flame's natural oscillating frequency and create complex nonlinear frequency components. A phase-locked PIV system is used to determine the flow characteristics for a propane-air flame. The results show that the effect of acoustic excitation on the flame dynamics decreases as the air-fuel flow rate is increased, because the combination of the initial flow velocity and the buoyancy effect of the flame counters the acoustic perturbation. Therefore, a chaotic flow pattern is only observed in the diffusion flame. In this case, the initial fuel velocity is low and the flame's hot gas flow simply follows the oscillation of the acoustic flow field. The vorticity contour maps match well with the velocity data, because the acoustic flow and the hot gas flow create opposing velocity components and form strong vortices.

This study demonstrates that the complex flame response complies with nonlinear theory and the observed frequency peaks are not random, but represent the nonlinear coupling modes of the excitation source and the flame instability oscillation. In acoustic excited flames, it can be shown that acoustic forcing results in response components at frequencies other than the excitation frequency. The observed nonlinear frequency modes are explained by nonlinear theory. An explanation of the physical mechanisms that are involved in the formation of these nonlinear frequency modes is given. For a practical combustion device, such as a gas turbine combustor, a study of the various frequency peaks and the relationships between them would be worthwhile.

Acknowledgement

References

[1] Chao, Y.-C. and Ming-Shan, J., *Behavior of the lifted jet flame under acoustic excitation,* Symposium (International) on Combustion 1992; 24: 333-340.

[2] Baillot, F. and Demare, D., *Physical mechanisms of a lifted nonpremixed flame stabilized in an acoustic field,* Combustion Science and Technology 2002; 174: 73-98.

[3] Toong, T.Y., Richard F, S., John M, S., and Griffin Y, A., *Mechanisms of combustion instability,* Symposium (International) on Combustion 1965; 10: 1301-1313.

[4] Demare, D. and Baillot, F., *Acoustic enhancement of combustion in lifted nonpremixed jet flames,* Combustion and Flame 2004; 139: 312-328.

[5] N. NOIRAY, D. DUROX, T. SCHULLER, and S. CANDEL, *A unified framework for nonlinear combustion instability analysis based on the flame describing function,* Journal of Fluid Mechanics 2008; 615: 139-167.

[6] Farhat, S.A., Ng, W.B., and Zhang, Y., *Chemiluminescent emission measurement of a diffusion flame jet in a loudspeaker induced standing wave,* Fuel 2005; 84: 1760-1767.

[7] Saito, M., Sato, M., and Nishimura, A., *Soot suppression by acoustic oscillated combustion,* Fuel 1998; 77: 973-978.

[8] Kim, K.T., Lee, J.G., Quay, B.D., and Santavicca, D.A., *Response of partially premixed flames to acoustic velocity and equivalence ratio perturbations,* Combustion and Flame 2010; 157: 1731-1744.

[9] Kartheekeyan, S. and Chakravarthy, S.R., *An experimental investigation of an acoustically excited laminar premixed flame,* Combustion and Flame 2006; 146: 513-529.

[10] Bourehla, A. and Baillot, F., *Appearance and Stability of a Laminar Conical Premixed Flame Subjected to an Acoustic Perturbation,* Combustion and Flame 1998; 114: 303-318.

[11] Williams, T.C., Shaddix, C.R., Schefer, R.W., and Desgroux, P., *The response of buoyant laminar diffusion flames to low-frequency forcing,* Combustion and Flame 2007; 151: 676-684.

[12] Huang, H.W., Wang, Q., Tang, H.J., Zhu, M., and Zhang, Y., *Characterisation of external acoustic excitation on diffusion flames using digital colour image processing,* Fuel 2012; 94: 102-109.

[13] Chen, L.W., Wang, Q., and Zhang, Y., *Flow characterisation of diffusion flame in a standing wave* Experimental Thermal and Fluid Science 2012; 41.

[14] Chen, L.W., *Flow Characterisation of Flames in an Acoustically Excited Chamber*, in *Department of Mechanical Engineering*. 2012, University of Sheffield, Sheffield. p. 214.

[15] Thompson, J.M.T. and Stewart, H.B., (2002) *Nonlinear Dynamics and Chaos*. Second Edition ed., Chichester, England: John Wiley & Sons, Ltd. p. 191.

[16]   Fenstermacher, P.R., Swinney, H.L., and Gollub, J.P., *Dynamical instabilities and the transition to chaotic taylor vortex flow,* Journal of Fluid Mechanics 1979; 94: 103-128.

Table

Table 1. Propane/air flow parameters in the experiment.

Equivalence ratio (Ø)	Air mass flow rate (kg/s)	Fuel mass flow rate (kg/s)	Air flow rate (ml/min)	Fuel flow rate (ml/min)	Velocity (m/s)
1.5	1.82×10^{-5}	1.75×10^{-6}	910	55	1.28
3	9.10×10^{-6}	1.75×10^{-6}	455	55	0.67
5	5.46×10^{-6}	1.75×10^{-6}	273	55	0.43

Figures
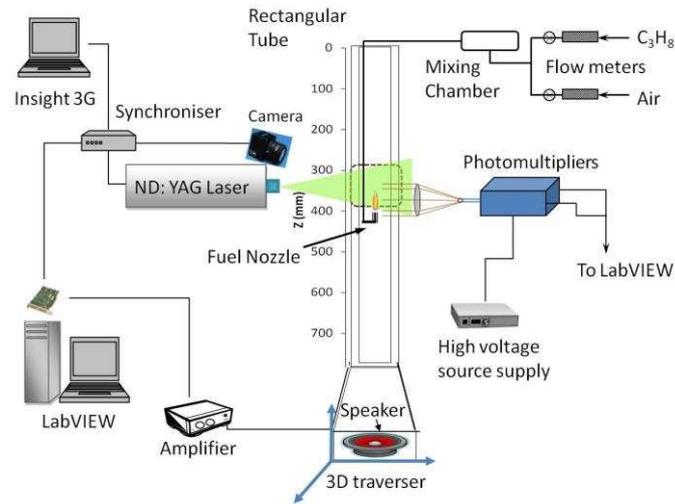
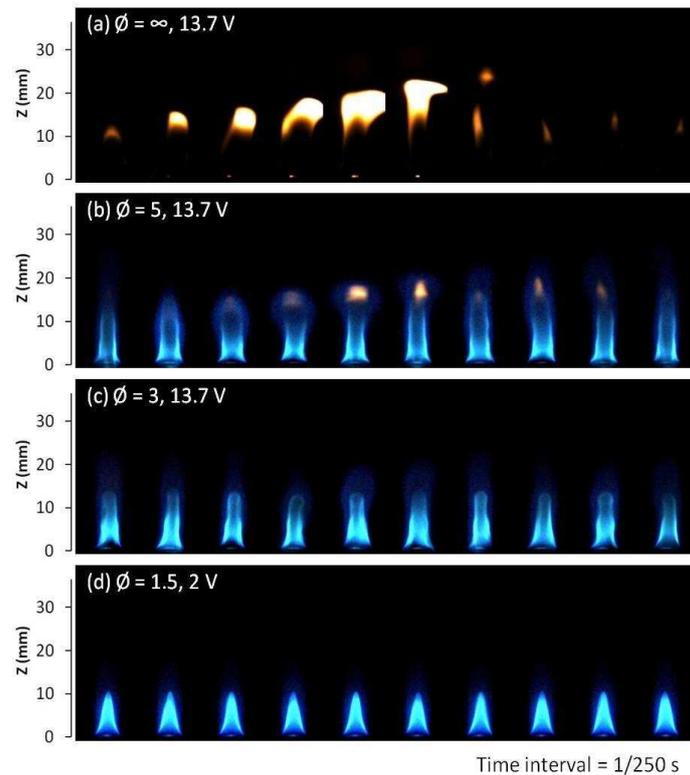Fig. 1. The schematic layout of the experimental apparatus.

Fig. 2. Propane-air flame images at different equivalence ratios and at the excitation frequency of
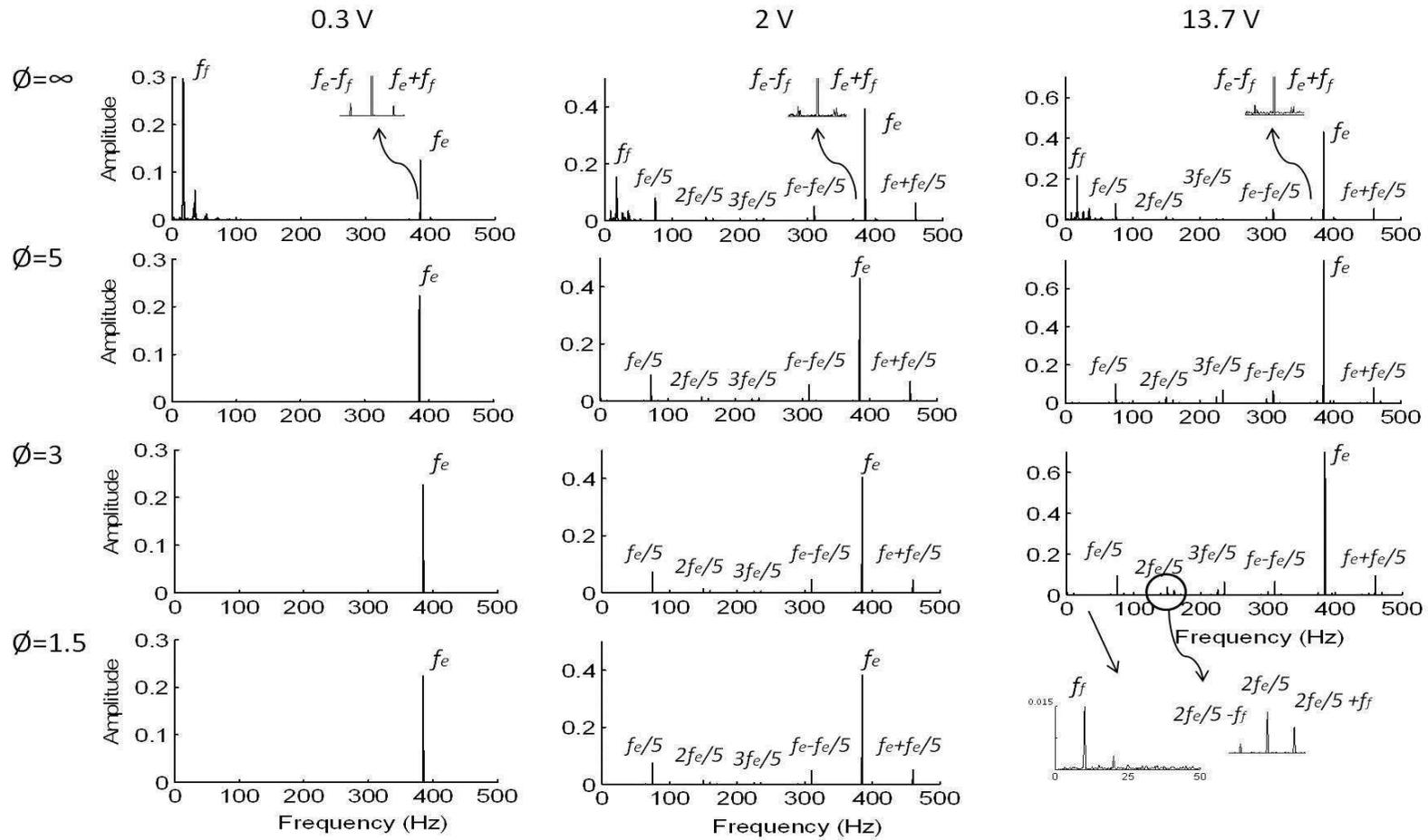
385 Hz.

Fig. 3. Power spectra of CH* chemiluminescence signals for for the premixed flames under acoustic excitation.
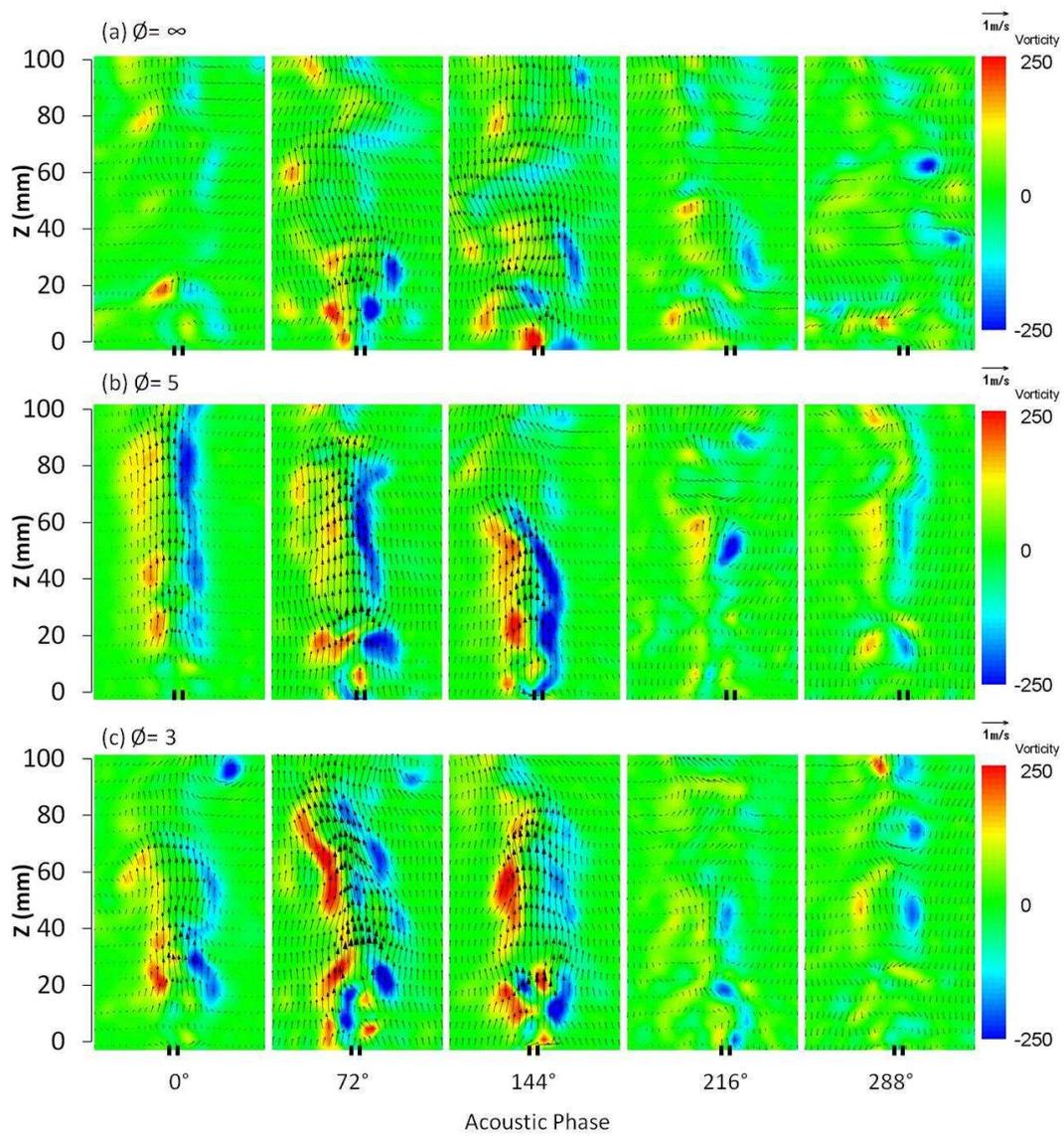
Fig. 4. Velocity vectors and the vorticity contour maps of the instantaneous propane-air flame flow

at the excitation frequency of 385 Hz